

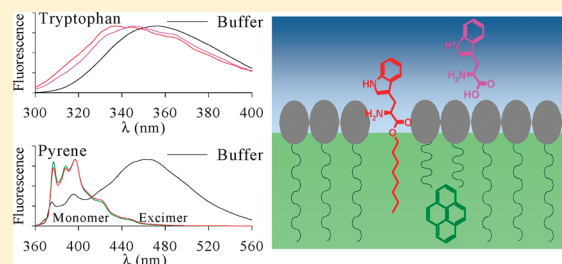
Characterization of the Head Group and the Hydrophobic Regions of a Glycolipid Lyotropic Hexagonal Phase Using Fluorescent Probes

N. Idayu Zahid,[†] Osama K. Abou-Zied,^{‡,*} Rauzah Hashim,[†] and Thorsten Heidelberg[†]

[†]Department of Chemistry, Faculty of Science, University of Malaya, 50603 Kuala Lumpur, Malaysia

[‡]Department of Chemistry, Faculty of Science, Sultan Qaboos University, P. O. Box 36, Postal Code 123, Muscat, Sultanate of Oman

ABSTRACT: Lyotropic liquid crystal phases are related to biological entities such as cell membranes, as well as to technological applications, for example, emulsifier and drug-delivery systems. We characterized here one of the most stable lyotropic phases of the β MaltoOC₁₂ lipid, the hexagonal phase (comprised of 65% (w/w) aqueous formulation of *n*-dodecyl β -D-maltoside), using fluorescent probes. Probing different parts of the polar head group region using tryptophan (Trp) and two of its ester derivatives (Trp-C₄ and Trp-C₈) indicates a polarity gradient. Both Trp and Trp-C₄ reside slightly away from the maltoside sugar units, and the local polarity is similar to that of simple alcohols (methanol and ethanol). For Trp-C₈, the long chain length pulls the Trp moiety closer to the head groups and the local polarity approaches that of 1,4-dioxane. The reduction in polarity indicates a smooth transition from the polar domain to the hydrophobic domain, which is important for the stability of the lipid. Two fluorescence lifetimes were measured for tryptophan and its derivatives in lipid. The results point to a degree of flexibility of the lipid self-assembly that allows the Trp side chain to adapt two different rotamers. Using pyrene to probe the hydrophobic region of the lipid self-assembly indicates the tendency of the pyrene molecules to disperse among the hydrophobic tails and to avoid dimerization. By comparing the measured ratio of the pyrene vibronic peak intensities (I_1/I_3) in lipid to that in buffer and in cyclohexane, it was concluded that pyrene must be close to the head groups. Two lifetime components were measured for pyrene in lipid which indicates a degree of heterogeneity in the pyrene local environment. Interaction between the C₈ chain of Trp-C₈ with pyrene is observed as a slight decrease in the I_1/I_3 ratio and the pyrene lifetime. The results presented here will be useful as a benchmark to utilize the present probes combination to characterize other biologically related lipid phases that are thought to play a crucial role in lipid–membrane interaction.



INTRODUCTION

Glycolipids (GLs) belong to a large family of molecules known as glycoconjugates.^{1–3} They have been extensively studied due to their connection to biological cell membranes. Although GLs are minor components in prokaryotes' and eukaryotes' cell membranes (compared to phospholipids), their widespread occurrence and extensive structural diversity suggest functional importance in cell processes^{4–10} such as endo- and exocytosis, apoptosis, and molecular recognition at the cell surface specific to the cell type.^{3,11,12} Chemically, GLs exhibit surfactant properties due to the dichotomic balance of the carbohydrate head group (with one or more monosaccharide units) and the lipophilic tail. As amphiphilic liquid crystals,^{13–16} they are able to self-assemble in both dry (thermotropic) and solvated (lyotropic) states into many different polymorphic forms such as the lamellar, hexagonal, sponge, and gel phases depending on appropriate conditions.

Phase studies of glycolipids have mostly focused on lyotropic systems because these are closely related to biological membranes. The adhesion property of the sugar head groups and their interactions with peptides and surface proteins make them suitable targets for nanoparticle vectors.¹⁷ Their importance in biology and industry has encouraged many synthetic glycolipids to be developed, including alkylpolyglucosides (APGs), which have been used for numerous surfactants applications.^{18–20}

In this paper, we characterize one of the glycoside systems, namely, the columnar phase of an aqueous formulation of the *n*-dodecyl β -D-maltoside (β MaltoOC₁₂) system (shown in Figure 1) using steady-state and time-resolved fluorescence methods. The lipid self-assembly structure and a partial phase diagram of β MaltoOC₁₂ have been reported previously.^{21,22} In water, β MaltoOC₁₂ gives a variety of self-assembly structures, including the hydrated solid, lamellar, cubic, and hexagonal phases, as well as the micellar solution as a function of increasing water concentration. β MaltoOC₁₂ has been used in many applications such as in the purification and stabilization of RNA polymerase,²³ protein solubilization,²⁴ and detection of protein–lipid on bacteriorhodopsin.²⁵ Herein, we study the β MaltoOC₁₂ hexagonal self-assembly structure, which exists over a wide range of concentration and temperature,²² at 65% (w/w) in aqueous formulation.

In the present study, we use two fluorescent probes, tryptophan and pyrene, as local reporters in the lipid. The former is used to probe the polar head group region and the latter to probe the hydrophobic region of the lipid. To access different regions in the hydrophilic domain, variable alkyl chains attached to the

Received: June 27, 2011

Revised: August 26, 2011

Published: August 30, 2011

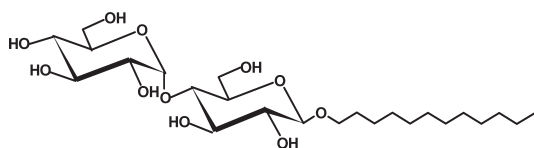


Figure 1. Chemical structure of *n*-dodecyl β -D-maltoside.

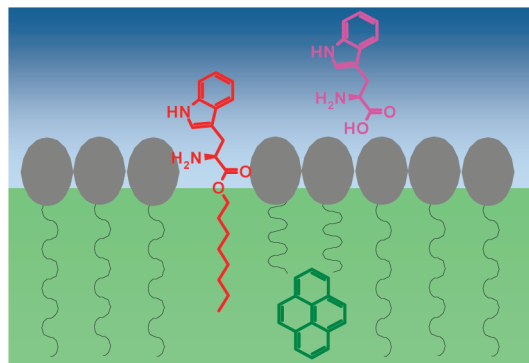


Figure 2. Schematic diagram showing one layer of the lipid self-assembly with the expected locations of the probes: pink, tryptophan (Trp); red, Trp-C8; green, pyrene.

tryptophan ester molecule were used, similar to the dynamics study reported by Kim et al.²⁶ A schematic diagram showing how the tryptophan molecule approaches the head groups with increasing alkyl chain length is given in Figure 2. Pyrene is expected to reside in the hydrophobic region as shown in the diagram. We estimate the polarity of different regions of the polar domain on the basis of a parallel study in different solvents, and we discuss our results in relation to the flexibility of the lipid self-assembly.

EXPERIMENTAL SECTION

Materials. β MaltoC₁₂ (98%) and pyrene (99%) were purchased from Sigma-Aldrich Chemical Co. L-Tryptophan (99%) was obtained from Merck. Tryptophan butyl ester (Trp-C₄) and its octyl analogue (Trp-C₈) used in this work were prepared according to a literature procedure.²⁷ Anhydrous 1,4-dioxane and methanol were obtained from Sigma-Aldrich. Anhydrous ethanol was received from Acros Organics. Spectroscopic grade cyclohexane was purchased from BDH Chemicals. Deionized water (Millipore) was used. All chemicals and solvents were used without further purification.

Sample Preparation. The concentration of tryptophan/tryptophan ester/pyrene in the aqueous β MaltoC₁₂ formulation for both steady-state and time-resolved experiments was adjusted to ~ 0.1 mM. The value is based on an estimated density of ~ 1.3 g mL⁻¹ for the mixture. The hexagonal phase used for this study was observed at 65% (w/w) aqueous formulation of β MaltoC₁₂ according to its published binary phase diagram.²² The hexagonal phase was confirmed using optical polarizing microscopy (OPM) by contact penetration. OPM investigations with water and buffer led to the same optical texture. All samples were prepared by mixing the lipids with tryptophan/tryptophan esters/pyrene dissolved in methanol. The methanol was evaporated afterward, and the samples were dried in a high vacuum to remove the solvent traces. A 65 mg amount of the mixture and 35 mg of

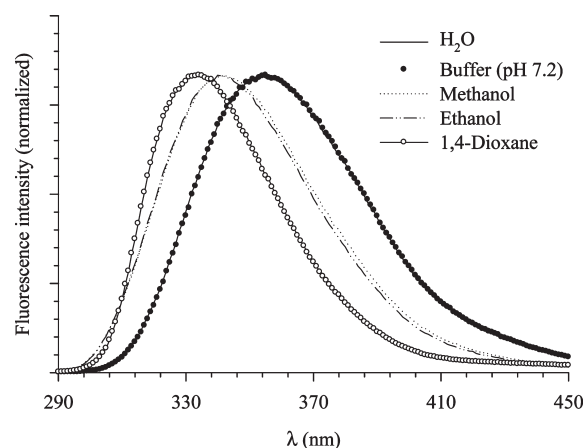


Figure 3. Fluorescence spectra of tryptophan in different solvents. $\lambda_{\text{ex}} = 280$ nm.

H₂O were placed in a 4 mm diameter quartz tube. The hydrated sample was immediately flame-sealed and underwent repeated cycles of centrifugation and heating to ensure that a homogeneous mixture was formed. As for reference samples in solution, all were prepared at a concentration of 0.05 mM. For samples which were difficult to dissolve in H₂O (tryptophan esters and pyrene), a stock solution in methanol (5 mM) was prepared. This solution was then diluted with aqueous buffer (25 mM sodium phosphate buffer, pH 7.2) to reach the desired concentration. The final methanol:H₂O (v/v) mixture was 10:90. A ratio above 20:80 was shown to behave like pure water.^{28–32}

Instrumentation. Fluorescence spectra were recorded on a Shimadzu RF-5301 PC spectrofluorophotometer. Lifetime measurements were performed using a TimeMaster fluorescence lifetime spectrometer obtained from Photon Technology International. Excitation was done at 280 and 340 nm using light-emitting diodes (LEDs). The instrument response function (IRF) was measured from the scattered light and estimated to be approximately 1.5 ns (full width at half-maximum (fwhm)). The measured transients were fitted to multiexponential functions convoluted with the system response function. The fit was judged by the value of the reduced χ^2 . The experimental time resolution (after deconvolution) was approximately 100 ps, using stroboscopic detection.³³ In all the experiments, samples were measured in a 1 cm path length quartz cell at 23 ± 1 °C.

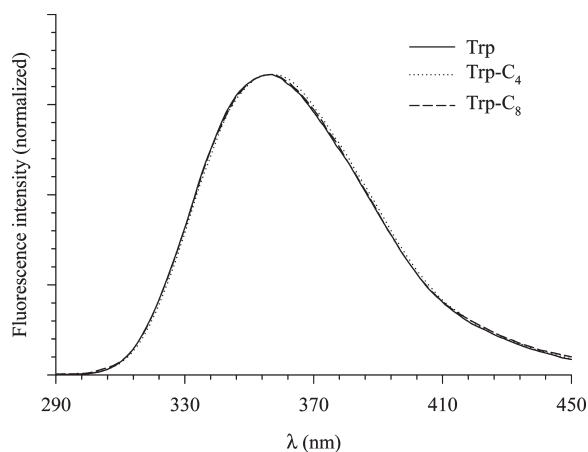
RESULTS AND DISCUSSION

Probing the Polar Region of the Lipid. To understand the spectroscopic behavior of the probes inside the glycolipids, it is important to understand how fluorescence from each probe is affected by its local environment. We start this section by discussing the fluorescence results of tryptophan in different solvents.

One factor affecting the tryptophan fluorescence is the polarity of its surrounding environment. The fluorescence spectrum of tryptophan is strongly dependent on solvent polarity. Figure 3 shows the fluorescence spectra of tryptophan in different solvents of varying polarity. Table 1 displays the position of the peak maxima. The sensitivity of the peak position is clearly dependent on the solvent polarity. In a solvent such as 1,4-dioxane (a non-dipolar solvent³⁴), fluorescence is peaked at 334 nm, whereas this peak is red-shifted as the solvent polarity increases. The maximum red shift is observed in aqueous solution. The detected

Table 1. Fluorescence Spectral Peak Positions of Trp and Its Derivatives in Different Solvents and Lipid

probe	solvent/medium	ϵ , ^a 25 °C	π^* , ^a	E_T^N , ^a 25 °C	peak max ^b (nm)
Trp	1,4-dioxane	2.21	0.49	0.16	334
	ethanol	24.55	0.54	0.65	340
	methanol	32.66	0.60	0.76	342
	buffer	78.30	1.09	1.00	355
	lipid				345
Trp-C ₄	buffer				355
	lipid				345
Trp-C ₈	buffer				355
	lipid				337

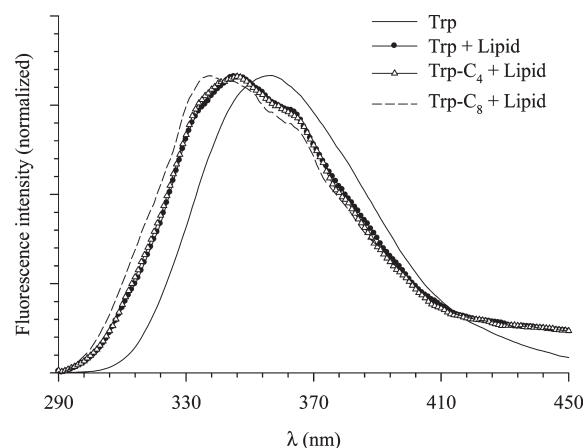
^a Obtained from ref 38. ^b $\lambda_{\text{ex}} = 280$ nm.**Figure 4.** Fluorescence spectra of tryptophan and its derivatives in buffer. $\lambda_{\text{ex}} = 280$ nm.

unstructured fluorescence in all of the solvents is due to the 1L_a state, since fluorescence from the 1L_b state is reported to be structured.^{35,36} The 1L_a state is more solvent-sensitive than the 1L_b state, and its transition shifts to lower energies in polar solvents.³⁷ The higher solvent sensitivity for the 1L_a state is expected since the 1L_a transition more directly involves the polar nitrogen atom of the indole ring of the tryptophan moiety.³⁷

We note here that the fluorescence peak in H₂O and buffer are the same with respect to shape and position, which indicates that there is no salt effect of the buffer on the 1L_a excited-state fluorescence of tryptophan. Figure 4 shows the fluorescence spectra of tryptophan and its two derivatives (Trp-C₄ and Trp-C₈) dissolved in buffer after excitation at 280 nm. As shown in the graph, the alkyl chain of the tryptophan ester has no effect on the fluorescence peak.

Figure 5 shows the fluorescence spectra of the three probes (Trp, Trp-C₄, and Trp-C₈) embedded in the lipid and measured after excitation at 280 nm. The fluorescence spectrum of Trp in buffer is included for comparison. As shown in the graph, the spectra in lipid are blue-shifted, compared to that in buffer. This observation is an indication of the different environment experienced by the tryptophan moiety in the polar region of the head groups of the lipid (being less polar compared to pure water). Table 1 summarizes the fluorescence peak maxima in buffer and lipid.

According to the results of Figure 5 and Table 1, the tryptophan molecule has a local environment that is less polar than bulk water.

**Figure 5.** Fluorescence spectra of tryptophan and its derivatives in lipid. The spectrum of tryptophan in buffer is included for comparison. The spectra are normalized for easy comparison. $\lambda_{\text{ex}} = 280$ nm.

As the chain length increases (see the case of Trp-C₈), the tryptophan molecule is pulled closer to the polar head groups and its fluorescence shows the most blue shift. This is due to the nature of the alkyl ester chain being hydrophobic and tending to escape the hydrophilic region. This tendency results in burying the chain inside the tail region of the lipid, which in turn brings the tryptophan molecule (attached to the chain) closer to the head groups. The pronounced blue shift observed in the case of Trp-C₈ indicates that water molecules are less polar as they get closer to the head groups. This observation complements earlier results, which show that water molecules tend to be more ordered and less flexible as they get closer to the head groups.²⁶ (This may explain the unique solvation characteristic of water that requires random distribution (disorder) of the water molecules in order to solvate the polar sites of the solute molecule, causing a maximum polarity effect.) The less flexible water molecules in the head group region may interrupt the tendency of water molecules to strongly associate with each other through intermolecular hydrogen bonds that allow more than one molecule of water to form a solvent network.³⁸ The constrained water molecules may cause the reduced polarity effect experienced by the tryptophan moiety.

By comparing the fluorescence peak position of tryptophan in lipid (Figure 5) and in different solvents (Figure 3), we may estimate the polarity of the local environment around the tryptophan moiety when embedded in lipid. The peak positions in the case of Trp and Trp-C₄ in lipid are close to that in methanol and ethanol (see Table 1). This indicates that the polarity of the intermediate region between bulk water and the head groups resembles that of simple alcohols (water in this region is more flexible than water at the head group region). On the other hand, as tryptophan gets closer to the head groups, it experiences a local polarity close to that of 1,4-dioxane (compare the peak position for Trp-C₈ in lipid with that in 1,4-dioxane).

Details about the physical nature of the head group region of the lipid system may be correlated to the physical properties of the 1,4-dioxane molecule as a solvent. A solvent such as 1,4-dioxane, which appears to be nonpolar according to its static dielectric constant ($\epsilon = 2.21$), has a high solvent polarity parameter ($\pi^* = 0.49$) and an E_T^N value of 0.16 (see Table 1).³⁸ 1,4-Dioxane has two CH₂–O–CH₂ groups opposite from each other, which results in a net zero dipole moment. Hence, it is considered a non-dipolar

Table 2. Fluorescence Lifetime (ns) Measurements of Trp and Its Derivatives in Buffer and Lipid

probe	buffer			lipid		
	τ_1^a	τ_2^b	χ^2	τ_1^a	τ_2^b	χ^2
Trp	0.55 (0.10)	3.9 (0.90)	1.05	0.17 (0.49)	3.7 (0.51)	1.03
Trp-C ₄	0.69 (0.15)	3.7 (0.85)	1.00	0.23 (0.46)	3.7 (0.54)	1.02
Trp-C ₈	0.45 (0.16)	3.8 (0.84)	1.01	0.17 (0.56)	3.8 (0.44)	1.00

^aUncertainty in measurements is ± 0.04 ns. ^bUncertainty in measurements is ± 0.1 ns. Emission was detected using a Schott WG-320 filter. Relative contributions are listed in parentheses. $\lambda_{\text{ex}} = 280$ nm.

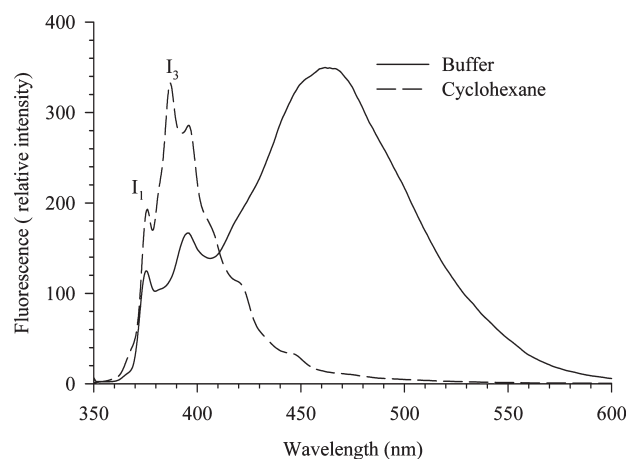
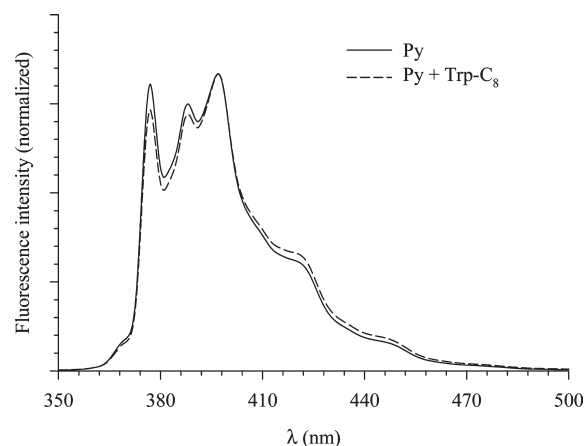
solvent.³⁴ However, 1,4-dioxane exhibits a large quadrupole moment,^{39,40} which is reflected in its π^* parameter that mainly takes into consideration the polarizability and the dipolarity of the solvent.³⁴ The corresponding E_T^N value indicates that 1,4-dioxane exhibits only 16% of the solvent polarity of water, thus classifying 1,4-dioxane as an apolar, non-hydrogen-bond donor solvent.³⁸ Water interaction with the head groups of lipid may resemble the interaction between 1,4-dioxane and water which are miscible in all proportions. Mixtures of 1,4-dioxane and water were proposed as media to study probes in nanoenvironments similar to those encountered in vesicles and at interfaces.^{28,29,41–44}

The above results point to a polarity gradient in the lipid self-assembly system. The reduction in polarity in going from the center of the hydrophilic region toward the head group region indicates a smooth transition from the polar domain to the hydrophobic domain, which is important for the stability of the lipid.

The fluorescence lifetimes of tryptophan and its ester derivatives were measured in buffer and lipid. The data are summarized in Table 2. The two measured lifetime components of tryptophan in buffer are due to two different rotamers.^{37,45} The relative contribution from the short-lifetime component increases in lipid. The biexponential nature of the Trp fluorescence decay in lipid constitutes strong support for the ground-state heterogeneity that is associated with a degree of flexibility of the Trp side chain to adapt two different rotamers. The results point to a degree of flexibility of the lipid self-assembly.

Probing the Hydrophobic Region of the Lipid. In this section, we investigate the tail region of the lipid by using pyrene as a probe. As a hydrophobic molecule, pyrene is expected to favor the tail region of the lipid assembly. We first show the fluorescence spectra of pyrene measured in buffer and in cyclohexane (Figure 6). The sharp and structured band (~ 360 – 450 nm) is due to the monomer fluorescence, whereas the unstructured band centered at ~ 465 nm is fluorescence from the pyrene excimer.^{37,46}

Pyrene tends to form excimers even at low concentrations. No excimers were detected in cyclohexane at $[\text{pyrene}] = 0.05$ mM as shown in Figure 6. In buffer, the hydrophobic nature of pyrene is expected to cause molecules to cluster close to each other in order to avoid the highly disliked polar nature of the solvent. This is manifested in the high yield of excimer formation at the same solvent:pyrene ratio. The structured fluorescence from the monomer species has two characteristic peaks with maxima at ~ 375 and ~ 385 nm (marked in Figure 6 as I_1 and I_3 , respectively). The ratio of the two peak intensities (I_1/I_3) is environmentally sensitive and has been used to elucidate the local environment of pyrene.^{47–49} An increase in the I_1/I_3 ratio is indicative of increased apparent polarity. This ratio is 0.58 in cyclohexane and 1.08 in buffer,⁵⁰ calculated from the spectra in Figure 6. The I_1/I_3

**Figure 6.** Fluorescence spectra of pyrene dissolved in buffer and cyclohexane. $\lambda_{\text{ex}} = 340$ nm.**Figure 7.** Fluorescence spectra of lipid containing pyrene (Py) and Py + Trp-C₈. $\lambda_{\text{ex}} = 340$ nm.

ratio along with the excimer fluorescence peak will be used as a benchmark when pyrene is complexed with lipid in order to predict the local environment around the pyrene molecule in lipid.

Figure 7 shows the fluorescence of pyrene in lipid and in lipid containing Trp-C₈. The results show that the excimer fluorescence is completely absent in lipid. This observation indicates that pyrene molecules are distributed among the tails of the lipid assembly and prefer to be isolated from each other (hydrophobic solvation). The I_1/I_3 ratio is calculated to be 1.04. The ratio is slightly less than that shown above for pyrene in buffer. We note here that the strong tendency to form excimers in buffer (vide supra) is expected to partially shield the pyrene molecule from complete exposure to water and hence lower the I_1/I_3 ratio. Also, using molecular dynamics simulation, it was shown in the lipid assembly (1-palmitoyl-2-oleoylphosphatidylcholine) that pyrene prefers a position inside the lipid membrane near the head groups.⁵¹ Although pyrene is a very hydrophobic molecule, it was found mainly in the highly ordered upper acyl chain region near the lipid head groups and not in the middle of the membrane, which is the most hydrophobic part. So, the I_1/I_3 ratio in our case indicates a similar situation in which the pyrene molecules may eventually be close to the polar region and yet hidden inside the tail region of the lipid.

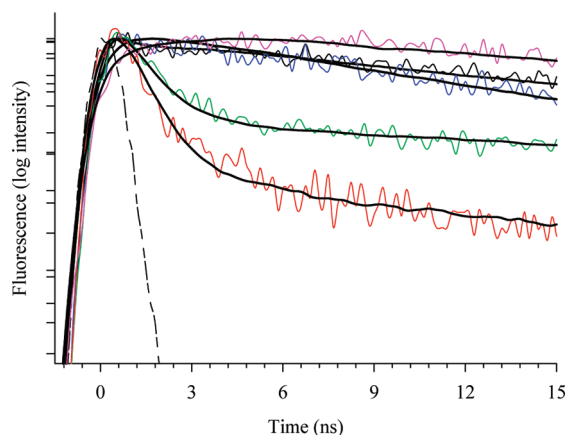


Figure 8. Fluorescence decay transients of pyrene probed using a Schott WG-380 filter: black, pyrene in buffer; blue, pyrene in buffer containing Trp-C₈; green, pyrene in lipid; red, pyrene in lipid containing Trp-C₈; pink, pyrene in buffer probed using a Schott WG-455 filter. $\lambda_{\text{ex}} = 340$ nm. IRF is shown by a dashed line.

Table 3. Fluorescence Lifetime (ns) Measurements of Pyrene and Pyrene with Trp-C₈ in Buffer and Lipid

probe	buffer		lipid		
	τ ^a	χ^2	τ_1 ^b	τ_2 ^a	χ^2
Py	28	1.02	0.97 (0.05)	51 (0.95)	1.07
Py + Trp-C ₈	22	1.12	0.97 (0.16)	27 (0.84)	1.40

^aUncertainty in measurements is ± 1 ns. ^bUncertainty in measurements is ± 0.05 ns. Emission was detected using a Schott WG-380 filter. Relative contributions are listed in parentheses. $\lambda_{\text{ex}} = 340$ nm.

The presence of Trp-C₈ causes a slight drop in the I_1/I_3 ratio to 1.02 (see Figure 7). The results indicate that the C₈ chain is indeed embedded inside the hydrophobic region of the lipid assembly. The presence of the C₈ chains inside the hydrophobic region may be a factor of increasing the hydrophobicity around the pyrene molecules. The incorporation of Trp-C₈ into the lipid layer may reduce the local polarity at the interface, which subsequently reduces the local polarity around the pyrene molecules.

Figure 8 and Table 3 summarize the fluorescence lifetime measurements of pyrene taken under air-saturated conditions. We measured a decay component of 29 ns for pyrene in buffer when probing the monomer emission. It was reported that the pyrene lifetime is very sensitive to the presence of oxygen in the sample.⁵² A decay component of 382 ns was reported in deoxygenated cyclohexane.⁵² In air-saturated cyclohexane, this decay component drops to 20 ns. In lipid, we measured a fast decay component of 0.97 ns and a slow decay component of 51 ns. The presence of two decay components reflects the heterogeneity in the local environment of pyrene inside the hydrophobic region. Comparing the long decay component with that in buffer, the value is almost doubled in lipid. This observation points to the cage effect of the hydrophobic tails in which pyrene is shielded from the solvent.

The pyrene lifetime in buffer is shorter when Trp-C₈ is present. The reduction in the lifetime is indicative of interaction between pyrene and Trp-C₈ in solution (Trp-C₈ is expected to act as a surfactant). Two decay components were again measured in lipid. The long decay component is much shorter than the

corresponding component measured for pyrene alone (27 vs 51 ns). The results indicate an interaction between the C₈ chain and pyrene inside the hydrophobic region, which is another confirmation that the C₈ chain indeed penetrates the tail region of the lipid and is in close proximity to pyrene.

Finally, a rise time of 10 ns was measured when probing the region of the excimer (455 nm and longer) for pyrene in buffer (see Figure 8). This lifetime is the time required for excimer formation. We did not detect any rise time for pyrene in the lipid which confirms the absence of excimers in the lipid assembly.

CONCLUSIONS

The hexagonal phase of the β MaltoOC₁₂ lipid, one of its most stable phases, was characterized here using fluorescent probes. The polar head group region was studied by following the change in fluorescence of tryptophan and two of its ester derivatives upon mixing with the lipid, while the hydrophobic region was investigated using pyrene. Comparing the fluorescence peak position of tryptophan in lipid and solution, we estimated the polarity of the region where Trp and Trp-C₄ reside to be close to that of simple alcohols (methanol and ethanol). Increasing the chain length attached to the tryptophan moiety to C₈ pulls the Trp molecule closer to the sugar groups and the local polarity approaches that of 1,4-dioxane. The reduction in polarity points to a smooth transition from the polar domain to the hydrophobic domain, which is important for the stability of the lipid. Two lifetimes were detected for the fluorescence decay of tryptophan and its derivatives in lipid. The results point to a degree of flexibility of the lipid self-assembly that allows the tryptophan side chain to adapt two different rotamers.

Comparing the fluorescence behavior of pyrene in solution and in lipid indicates the tendency of the pyrene molecules to disperse among the tails of the hydrophobic region as monomers. The ratio of I_1/I_3 implies that pyrene is close to the head groups. Interaction between pyrene and the C₈ chain of Trp-C₈ inside the hydrophobic region is observed as a slight reduction in the I_1/I_3 ratio and in the pyrene lifetime.

The results in this paper will be used as a benchmark to investigate other biologically related lipid phases, particularly the bicontinuous cubic phase, that are thought to play a crucial role in lipid–membrane interaction. This study is underway in our laboratories.

AUTHOR INFORMATION

Corresponding Author

*Tel.: (+968) 2414-1468. Fax: (+968) 2414-1469. E-mail: abouzed@squ.edu.om.

ACKNOWLEDGMENT

We thank the Brain-Gain Malaysia program under the Ministry of Science, Technology and Innovation (Grant No. 53-02-03-1040), University of Malaya (Grant No. UM.C/625/1/HIR/MOHE/05), and Sultan Qaboos University for financial support.

REFERENCES

- (1) *Novel Surfactants: Preparation, Applications, and Biodegradability*; Holmberg, K., Ed.; Marcel Dekker: New York, 2003.
- (2) *Sugar-Based Surfactants: Fundamentals and Applications*; Ruiz, C. C., Ed.; CRC Press/Taylor & Francis: Boca Raton, FL, USA, 2008.

- (3) *Glycolipids: New Research*; Sasaki, D., Ed.; Nova Science: New York, 2008.
- (4) Dembitsky, V. M. *Lipids* **2004**, *39*, 933–953.
- (5) Dembitsky, V. M. *Chem. Biodiversity* **2004**, *1*, 673–781.
- (6) Dembitsky, V. M. *Lipids* **2005**, *40*, 869–900.
- (7) Dembitsky, V. M. *Lipids* **2005**, *40*, 641–660.
- (8) Dembitsky, V. M. *Lipids* **2005**, *40*, 535–557.
- (9) Dembitsky, V. M. *Lipids* **2005**, *40*, 219–248.
- (10) Dembitsky, V. M. *Lipids* **2006**, *41*, 1–27.
- (11) Ernst, B.; Hart, G. W.; Sinaÿ, P. *Carbohydrates in Chemistry and Biology*; Wiley-VCH: Weinheim, Germany, 2000; Vol. 1.
- (12) *Glycolipids, Phosphoglycolipids, and Sulfoglycolipids, Handbook of Lipid Research*; Kates, M., Ed.; Plenum Press: New York, 1990; Vol. 3.
- (13) Jeffrey, G. A. *Acc. Chem. Res.* **1986**, *19*, 168–173.
- (14) Jeffrey, G. A.; Maluszynska, H. *Carbohydr. Res.* **1990**, *207*, 211–219.
- (15) Vill, V.; Hashim, R. *Curr. Opin. Colloid Interface Sci.* **2002**, *7*, 395–409.
- (16) Vill, V.; Böcker, T.; Thiem, J.; Fischer, F. *Liq. Cryst.* **2006**, *33*, 1351–1358.
- (17) Corti, M.; Cant, L.; Brocca, P.; Del Favero, E. *Curr. Opin. Colloid Interface Sci.* **2007**, *12*, 148–154.
- (18) von Rybinski, W.; Hill, K. *Angew. Chem., Int. Ed.* **1998**, *37*, 1328–1345.
- (19) Balzer, D.; Harald Lüders, H. *Nonionic Surfactants: Alkyl Polyglucosides*, Surfactant Science Series; Marcel Dekker: New York, NY, USA, and Basel, Switzerland, 2000; Vol. 91.
- (20) Zhang, R.; Zhang, L.; Somasundaran, P. *J. Colloid Interface Sci.* **2004**, *278*, 453–460.
- (21) Warr, G. G.; Drummond, C. J.; Grieser, F.; Ninham, B. W.; Evans, D. F. *J. Phys. Chem.* **1986**, *90*, 4581–4586.
- (22) Auvray, X.; Petipas, C.; Dupuy, C.; Louvet, S.; Anthore, R.; Rico-Lattes, I.; Lattes, A. *Eur. Phys. J. E* **2001**, *4*, 489–504.
- (23) Bujarski, J.; Hardy, S.; Miller, W.; Hall, T. *Virology* **1982**, *119*, 465–473.
- (24) Lambert, O.; Levy, D.; Ranck, J. L.; Leblanc, G.; Rigaud, J. L. *Biophys. J.* **1998**, *74*, 918–930.
- (25) Sasaki, T.; Demura, M.; Kato, N.; Mukai, Y. *Biochemistry* **2011**, *50*, 2283–2290.
- (26) Kim, J.; Lu, W.; Qiu, W.; Wang, L.; Caffrey, M.; Zhong, D. *J. Phys. Chem. B* **2006**, *110*, 21994–22000.
- (27) Li, J.; Sha, Y. *Molecules* **2008**, *13*, 1111–1119.
- (28) Abou-Zied, O. K. *J. Photochem. Photobiol., A* **2006**, *182*, 192–201.
- (29) Abou-Zied, O. K. *Chem. Phys.* **2007**, *337*, 1–10.
- (30) Andrade, S. M.; Costa, S. M. B. *Phys. Chem. Chem. Phys.* **1999**, *1*, 4213–4218.
- (31) Casassas, E.; Fonrodona, G.; Juan, A. J. *Solution Chem.* **1992**, *21*, 147–162.
- (32) Cheong, W. J.; Carr, P. W. *Anal. Chem.* **1988**, *60*, 820–826.
- (33) James, D. R.; Siemiarz, A.; Ware, W. R. *Rev. Sci. Instrum.* **1991**, *63*, 1710–1716.
- (34) Reichardt, C. *Chem. Rev.* **1994**, *94*, 2319–2358.
- (35) Pierce, D.; Boxer, S. *Biophys. J.* **1995**, *68*, 1583–1591.
- (36) Callis, P. R.; Burgess, B. K. *J. Phys. Chem. B* **1997**, *101*, 9429–9432.
- (37) Lakowicz, J. *Principles of Fluorescence Spectroscopy*; Springer Verlag: New York, 2006.
- (38) Reichardt, C. *Solvents and Solvent Effects in Organic Chemistry*, 3rd ed.; Wiley-VCH: Weinheim, Germany, 2003.
- (39) Suppan, P. *J. Photochem. Photobiol., A* **1990**, *50*, 293–330.
- (40) Suppan, P. *J. Lumin.* **1985**, *33*, 29–32.
- (41) Abou-Zied, O. K.; Al-Shihi, O. I. K. *Phys. Chem. Chem. Phys.* **2009**, *11*, 5377–5383.
- (42) Melo, E. C. C.; Costa, S. M. B.; Maçanita, A. L.; Santos, H. *J. Colloid Interface Sci.* **1991**, *141*, 439–453.
- (43) Belletete, M.; Lachapelle, M.; Durocher, G. *J. Phys. Chem.* **1990**, *94*, 5337–5341.
- (44) Belletete, M.; Lessard, G.; Durocher, G. *J. Lumin.* **1989**, *42*, 337–347.
- (45) Abou-Zied, O. K.; Al-Shihi, O. I. K. *J. Am. Chem. Soc.* **2008**, *130*, 10793–10801.
- (46) Kinnunen, P. K. J.; Koiv, A.; Mustonen, P. In *Fluorescence Spectroscopy: New Methods and Applications*; Wolfbeis, O. S., Ed.; Springer-Verlag: New York, 1993; pp 159–171.
- (47) Saxena, R.; Shrivastava, S.; Chattopadhyay, A. *J. Phys. Chem. B* **2008**, *112*, 12134–12138.
- (48) Ioffe, V.; Gorbenco, G. P. *Biophys. Chem.* **2005**, *114*, 199–204.
- (49) Haque, M. E.; Ray, S.; Chakrabarti, A. *J. Fluorescence* **2000**, *10*, 1–6.
- (50) The peak at 385 nm completely disappeared in buffer, so we took the intensity at this position which puts an upper limit for the I_3 value. This means that the calculated I_1/I_3 ratio of 1.08 may in fact be much higher.
- (51) Hoff, B.; Strandberg, E.; Ulrich, A. S.; Tieleman, D. P.; Posten, C. *Biophys. J.* **2005**, *88*, 1818–1827.
- (52) Karpovich, D. S.; Blanchard, G. J. *J. Phys. Chem.* **1995**, *99*, 3951–3958.